Copyright © 2017 Tech Science Press CMC, vol.53, no.2, pp.109-127, 2017

# Influence of functionalization on the structural and mechanical properties of graphene

**L.S. Melro[1,2] and L.R. Jensen[1]**

**Abstract**: Molecular dynamics simulations were applied in order to calculate the Young's modulus of graphene functionalized with carboxyl, hydroxyl, carbonyl, hydrogen, methyl, and ethyl groups. The influence of the grafting density with percentages of 3, 5, 7, and 10% and the type of distribution as a single cluster or several small clusters were also studied. The results show that the elastic modulus is dependent on the type of functional groups. The increasing coverage density also evidenced a decrease of the Young's modulus, and the organization of functional groups as single cluster showed a lesser impact than for several small clusters. Furthermore, the bond length and angle distribution probability analyses reveal that lengths and angles are affected with increasing functionalization suggesting more out-of-plane displacements of the carbon atoms within the graphene structure.

**Keywords**: Functionalization, graphene, molecular dynamics, Young's modulus, structural properties

## 1 Introduction

Graphene has attracted a vast interest owing to its outstanding mechanical [Lee, Wei, Kysar and Hone (2008); Xie, Wang and Zhang (2015)], thermal [Balandin, Ghosh, Bao, Calizo, Teweldebrhan, Miao and Lau (2008)] and electronic properties [Castro Neto, Guinea, Peres, Novoselov and Geim (2009)]. Structurally, it is a monolayer of carbon atoms covalently bonded by sp2-hybridized electrons in a hexagonal pattern. The length of a carbon-carbon bond is typically 1.42 Å, the bond angle 120 º, and the layer thickness 3.4 Å [Tsai and Tu, (2010)]. Chemical functionalization of graphene has been studied with relevance to hydrogen storage when functionalized with hydrogen atoms [Lin, Ding and Yakobson (2008)], for application as reinforcing fillers in composite materials [Ramanathan, Abdala, Stankovich, Dikin, Herrera-Alonso, Piner, Adamson, Schniepp, Chen, Ruoff, Nguyen, Aksay, Prud'Homme and Brinson (2008)] and for water filtration, namely desalination [Devanathan, Chase-Woods, Shin and Gotthold (2016)].

The mechanical properties of graphene have been investigated by a variety of simulation methods, from density functional theory [Van Lier, Van Alsenoy, Van Doren and Geerlings (2000)], to molecular mechanics [Chang and Gao (2003)] and molecular dynamics (MD) [Tsai and Tu, (2010); Zhou, Wang and Cao (2013); Javvajia, Budarapub, Sutrakarc, Roy Mahapatraa, Paggi,

[1] Department of Materials and Production, Aalborg University, Aalborg, Denmark.

[2] Corresponding author: liliana@m-tech.aau.dk.

Zi and Rabczukef (2016); Hou, Zhu, Liu, Dai, Liu, Wu and Zhang (2017); Liu and Yand (2017); Das and Ghosh (2017)]. Most studies regarding the mechanical properties of pristine and functionalized graphene focus on molecular dynamic simulations [Pei, Zhang and Shenoy (2010a, b); Zheng, Geng, Wang, Li and Kim (2010)]. Tsai and Tu (2010) studied the mechanical properties of pristine graphene by applying uniaxial tensile loading to the atomistic structures to calculate the Young's modulus and Poisson's ratio. Zhou, Wang and Cao (2013) also applied uniaxial stretching to study the in-plane elastic properties of single layer graphene with different chirality angles. In a similar study Yu, Chen, Cheng and Chen (2016) presented the effects of temperature, size, chirality and number of stacked layers on the aforementioned properties. The presence of vacancy and Stone-Wales defects on graphene and their effect on the Young's modulus was presented on a study by Jing, Xue, Ling, Shan, Zhang, Zhou and Jiao (2012).

The influence of functionalization was analyzed by Pei, Zhang and Shenoy (2010b) where they compared the mechanical properties of pristine, 10% and 100% hydrogen coverage graphene layers. A study by Pei, Zhang and Shenoy (2010a) focuses on the effect of location, distribution, and coverage density of methyl groups. The degree of functionalization, molecular structure and weight effect on the Young's modulus was studied by Zheng, Geng, Wang, Li and Kim (2010).

In the present work, we considered the influence of different functional groups (carboxyl, carbonyl, hydroxyl, methyl, ethyl, and hydrogen) as well as the coverage density and distribution of functional groups on the elastic modulus of graphene. A structural analysis was also performed to study how bond lengths and angles are affected by the functionalization and, in the case of hydroxyl functionalized graphene, how the lengths and angles relate to the deformation mechanisms of the graphene.

## 2 Simulation approach

### *2.1 Models development*

Graphene models were built using Materials Studio 6.0 [Accelrys Software Inc. Materials Studio v6.0.0. (2011)]. A single graphene layer consisting of 960 atoms was modelled with the dimensions 5.1 x 4.9 x 0.34 nm. Specific functional groups (-COOH, -C=O, -OH, -H, $-CH_3$, $-CH_2CH_3$) were individually and randomly grafted onto the graphene layer with 10% functionalization equivalent to 96 groups (Figure 1).

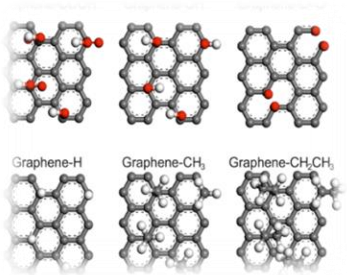


**Figure 1:** Excerpts of functionalized graphene models with 10% coverage of functional groups.

In order to study the influence of grafting density on the mechanical properties of graphene,

hydroxyl groups were randomly attached to the hexagonal structures in different percentages, as exemplified in Figure 2.

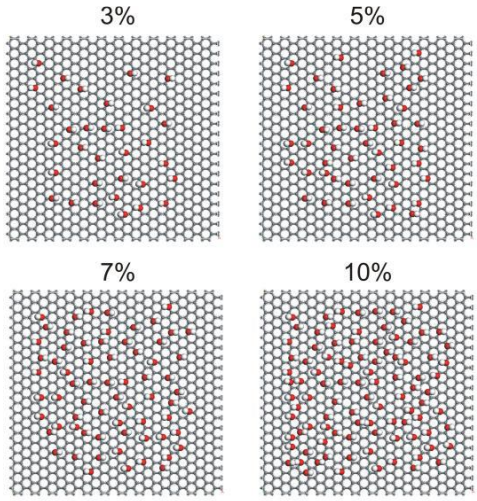


**Figure 2:** Models with 3, 5, 7, and 10% of hydroxyl functional groups.

The effect of the type of distribution of hydroxyl groups was assessed by comparing models with a single cluster and several small clusters. The study was performed for 3% and 10% functionalized layers (Figure 3).

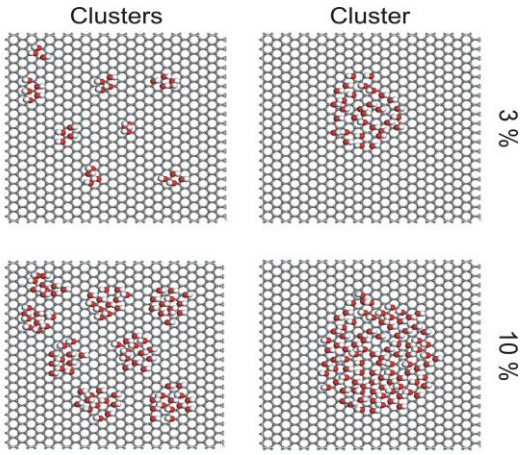


**Figure 3:** Hydroxylated graphene models of small clusters and one big cluster with 3% and 10% of functionalization.

### *2.2 MD simulations*

The Condensed-phase Optimized Molecular Potential for Atomistic Simulation Studies (COMPASS) force field was used to model the interactions between atoms. The COMPASS force field has been parametrized and validated to model the interaction of e.g. carbon, oxygen and hydrogen atoms in the hybridization states relevant for the graphene system

and the functional groups examined in this study [Sun (1998)]. The force field has been widely employed in simulations of graphene alone and together with other carbon-based materials [Jing, Xue, Ling, Shan, Zhang, Zhou and Jiao (2012); Lv, Xue, Xia, Ma, Xie and Chen (2010); Yu, Yang and Cho (2009); Zhou, Xue, Wang and Cao (2013); Guo, Montgomery Pettitt, and Wheeler (2006)]. The non-bonded interaction was calculated using the atom-based summation method with a cut-off radius of 9 Å.

All molecular models were equilibrated through geometry optimization using a combination of the steepest decent and the conjugate gradient methods followed by equilibration dynamic simulations. The equilibration dynamic simulation was performed in a NVT ensemble with the Nosé-Hoover-Langevin (NHL) thermostat for 100 ps and a time step of 1 fs. The simulations were performed at 1 K in order to minimize the effect of thermal vibrations. The equilibrated graphene systems were unidirectional strained in steps of 0.5% strain with a 100 ps dynamic simulation following each strain step. The parameters of the simulations were identical to the parameters used for the equilibration dynamics. From each strain step, the strain energy was determined as the potential energy difference between the unstrained system and the strained system. The strain energies are plotted as a function of strain and the Young's Modulus of the different systems is determined through the second derivative of best fits of the strain energy vs. strain curves [Agrawal, Sudalayandi, Raff and Komanduri (2006)] as shown in equation 1:

$$E = \frac{1}{V}\frac{\partial^2 U}{\partial^2 \varepsilon} \tag{1}$$

Where E is the Young's modulus, ε is the strain, U(ε) is the best fit function of the strain energy curves and V is the volume of the systems based on the dimensions of the graphene sheet (5.2 x 5.1 x 0.3 nm).

The structural properties of the graphene sheets were assessed by calculating the probability of bond length and angle distributions of the bonds belonging to the graphene sheet after the dynamics simulations. The bonds belonging to the functional groups were not included in these distributions.

## 3 Results and discussion

### *3.1 Structural properties*

Bond length distributions for the different functional groups, density and distribution are presented in Figures 4, 5 and 6, respectively. Pristine graphene presents three peaks, two of them at 1.40 Å and 1.42 Å, and a more intense at 1.41 Å. These values are close to the theoretical carbon-carbon bond length of 1.42 Å [Tsai and Tu (2010)]. The slight difference is attributed to a change in conformation of the system to reach a more favorable energetic state, and to some degree due to temperature effects. Differently, the functionalized graphene systems present a broader range of bond length distributions alike for all functional groups except carbonyl as shown in Figure 4. They present similar curve distributions that range from 1.39 to 1.43 Å. These distances are attributed to the carbon-carbon bonds that are not directly bonded to grafted carbons. The wider curves from 1.48 to 1.54 Å are a result of the bonds between grafted and neighboring carbon atoms. This is possibly due to the out-of-plane displacement of the grafted carbons which result in an elongation of these bonds.

The -$CH_2CH_3$ functionalized graphene layer presents longer bond lengths, followed by the -COOH and-$CH_3$ layers. The -OH and-H graphene layers present identical curves and at lower distances than the previous chemical groups, with the -H having an only slightly narrower curve. This suggests that the number of atoms that belong to the functional groups influence the bond length of the nearest atoms in the graphene sheet with the largest functional groups resulting in the largest bond lengths. Carbonyl presents a single, wider and less intense curve between 1.38 and 1.48 Å. In this case, the different bond lengths cannot be specifically attributed to functionalized or non-functionalized carbon-carbon bonds as there is no pattern to characterize them, unlike for the previous models.

The effect of grafting density is also visible on the bond length distributions, as can be seen in Figure 5. The larger the density coverage of functional groups the less intense and wider are the peaks between 1.39 and 1.43 Å meaning a broader distribution of the bond length. A second and less intense peak, which is attributed to the direct bond between grafted and neighboring carbon atoms, is present between 1.48 to 1.53 Å. This peak is does not change position in the case of 3, 5 and 7% but in the case of the 10% system a minor shift to lower lengths is observed indicating that the grafting density might influence the bond length if a certain threshold is exceeded. Further studies have to be performed to investigate this effect more thoroughly.

The influence of the distribution of the functional groups is presented in Figure 6 and shows that a higher bond length is obtained in the region between 1.49 Å and 1.54 Å if the functional groups are collected in a number of small clusters compared to assembling the groups in one single cluster. This is probably the same effect observed for the system with 10% grafting density where the influence of the functional groups on the closest carbon atoms is influenced when the groups are close to each other with the single cluster being an extreme case.

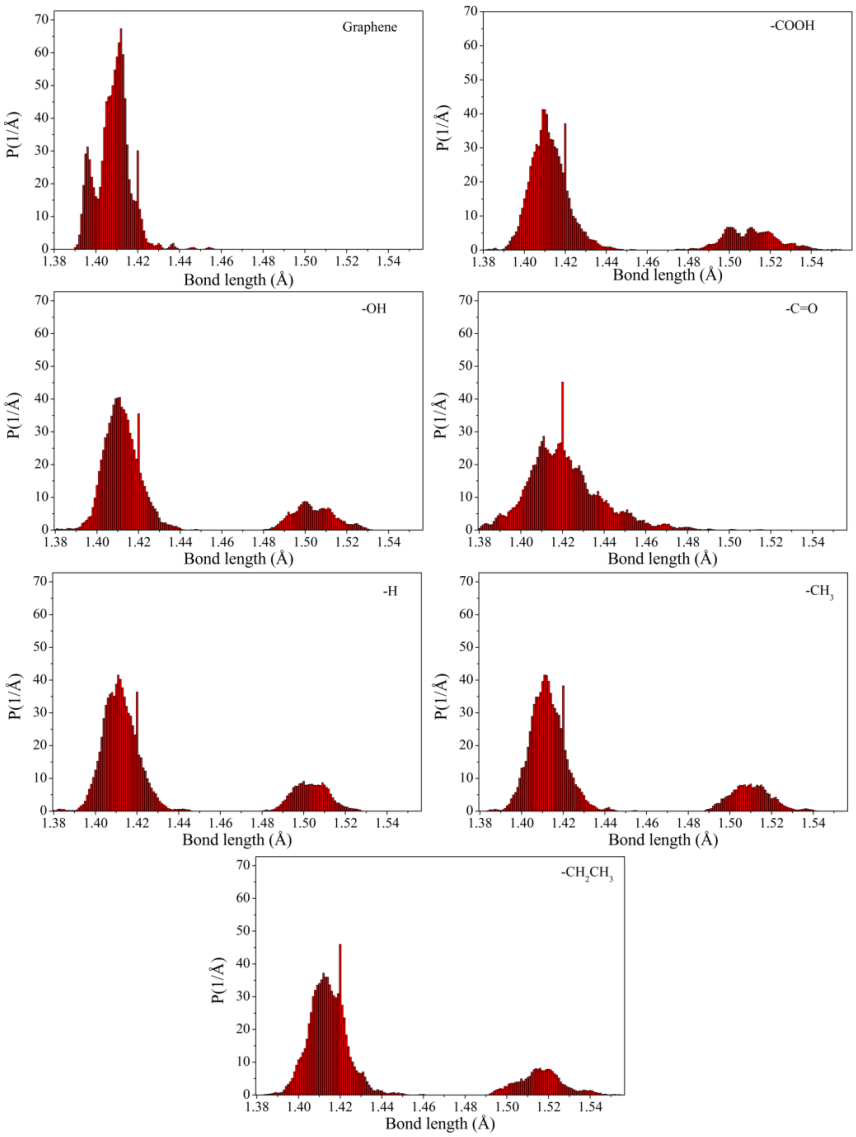


**Figure 4:** Bond length distribution for the functionalized graphene models after equilibration.

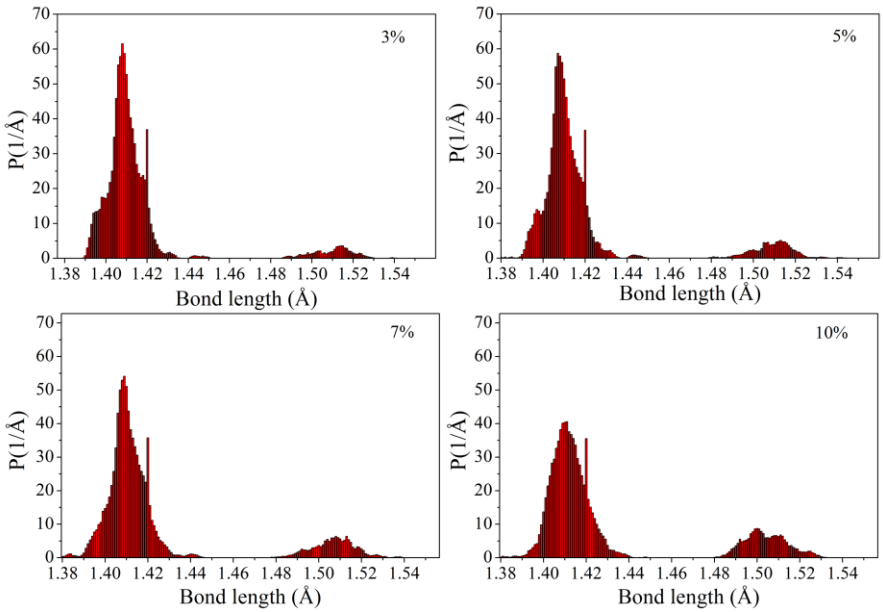


**Figure 5:** Bond length distribution for graphene with 3, 5, 7, and 10% coverage density of hydroxyl groups after equilibration.

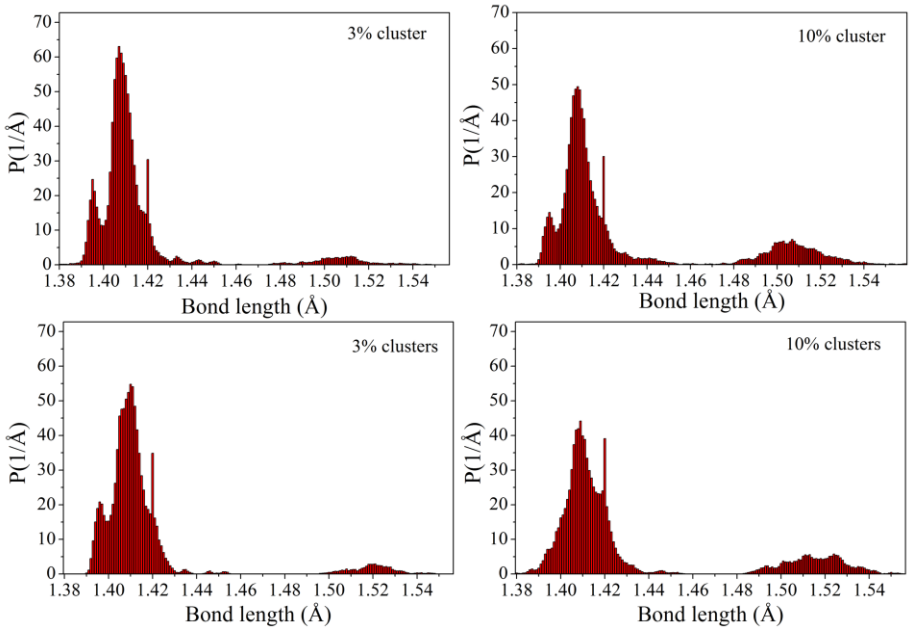


**Figure 6:** Bond length distribution for graphene with hydroxyl groups distributed in small clusters and as a single cluster for 3% and 10% grafting after equilibration.

The bond angle distribution plot for the pristine and the functionalized graphene is presented in Figure 7. The pristine graphene shows a bond angle varying between 117 ºand 123 º with one distinct peak at 119 ° and another with lower intensity at 122 º. The functionalized graphene present broader and lower intensity peaks varying between 116 ° and 124 ° with the carbonyl model presenting a curve slightly lower and broader than the remaining. The distribution plots of the functionalized systems also show that these systems have a further peak between 111 º and 116 º that is related to the grafted carbon atoms in the graphene sheets. The larger functional groups such as-$CH_2CH_3$, -COOH and -$CH_3$ have lower angle values than the remaining groups. A similar influence was observed for the bond length distribution as mentioned previously.

With an increase of functionalization density (Figure 8) the two peaks between 118 ° and 123 ºbecome less intense and less defined tending to merge into a single peak. On the other hand, the peak between 111 º and 116 º, that is observed for the grafted carbons in the graphene sheet, increase intensity with increasing functional groups.

The bond angle distribution plot for the different types of functional group distribution is presented in Figure 9. No clear influence of the distribution of the groups on the bond angles are observed.

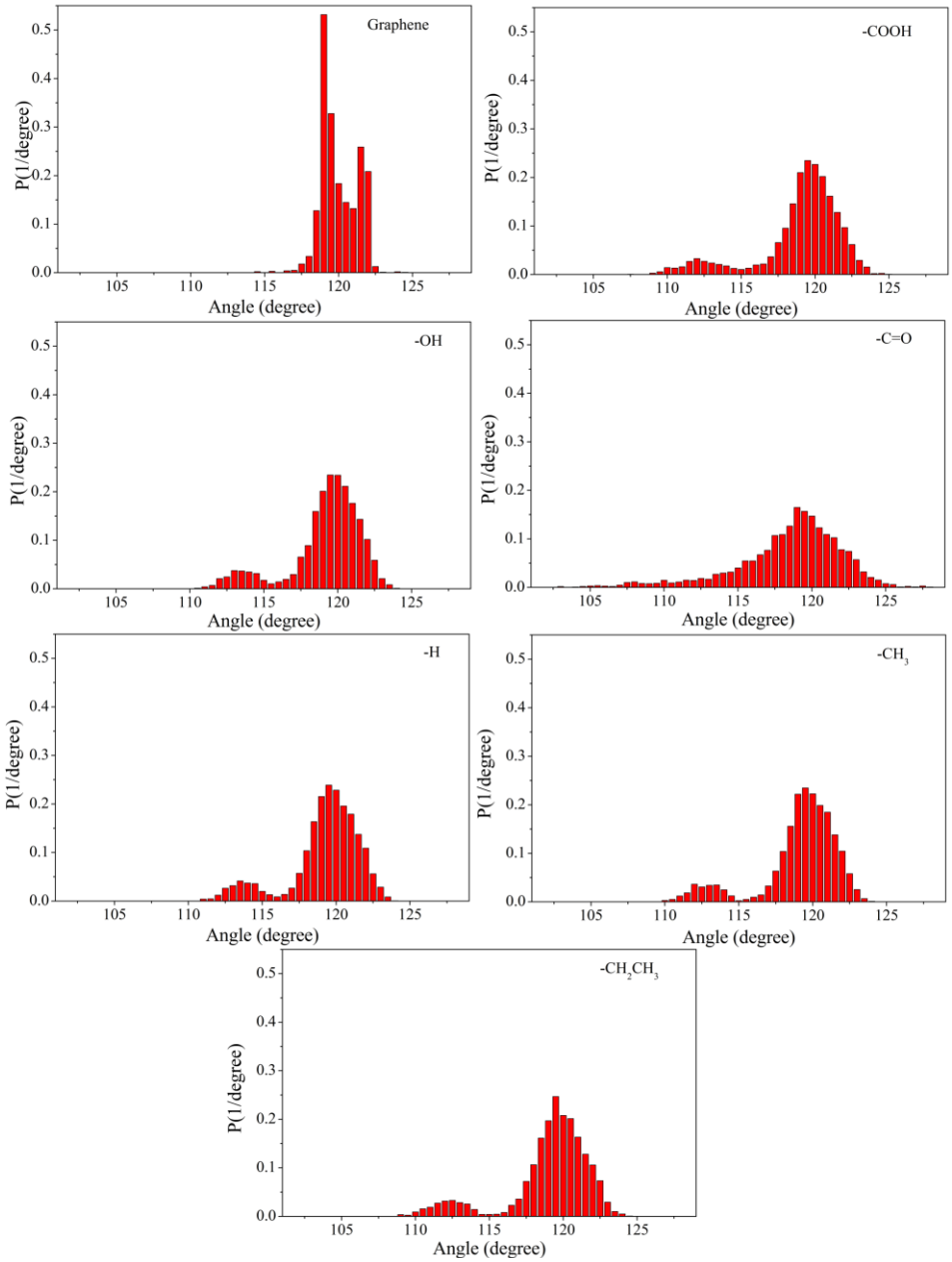


**Figure 7:** Angle distribution for graphene with different functional groups after equilibration.

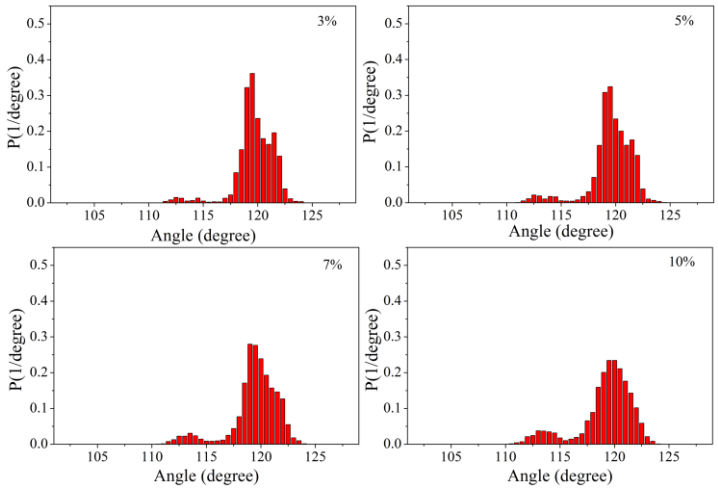


**Figure 8:** Angle distribution for graphene with 3, 5, 7, and 10% of hydroxyl groups after equilibration.

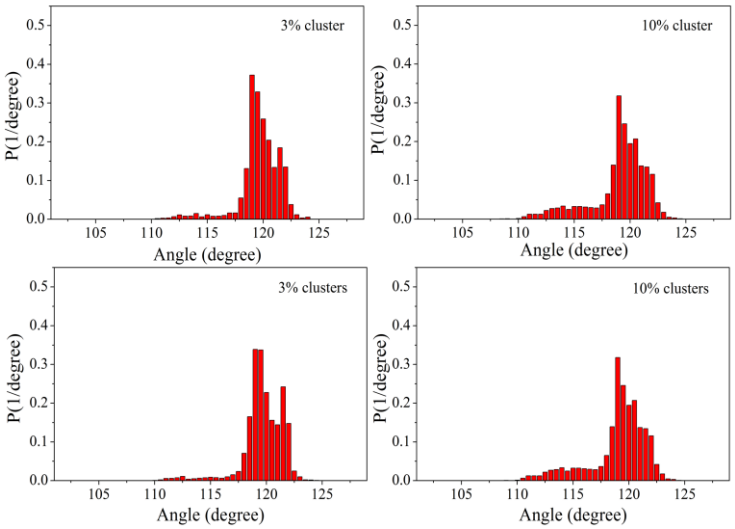


**Figure 9:** Angle distribution of graphene with hydroxyl groups distributed in small clusters and as a single cluster for 3% and 10% grafting after equilibration.

To study the deformation mechanisms of pristine and functionalized graphene systems the distribution plots of both the bond lengths and angles of pristine and OH-functionalized graphene systems are presented in Figures 10 and 11, respectively, for 0% and 5% strain. The bonds are colored according to the distribution plots and the red dots on the OH-functionalized graphene indicate the grafting sites.

The pristine graphene at zero strain presents three main bond distributions at 1.40, 1.41 and

1.42 Å. With applied strain higher bond length distributions appear at 1.46 Å which relate to the bonds affected by the direction of the strain. On the other hand, the bonds that are not influenced by the strain direction have approximate values from the structure with no strain applied, 1.39 Å. The graphene-OH system shows two distinct curves, the first within a similar range as the pristine graphene with no applied strain, which relates to the bonds whose carbon atoms are not directly connected to functional groups. And another between at higher bond lengths that according to the figure relate directly to the functionalized carbons. With applied strain the bonds that are not affected by the strain direction are found primarily at 1.39 Å, except if the bond is part of a carbon atom connected to a functional group, which in that case increases its length to 1.44 Å. The bonds affected by the strain direction also increase length to 1.44 Å when either of the two carbons that form the bond are connected to a functional group, and to 1.56 Å when

connected to a functional group.

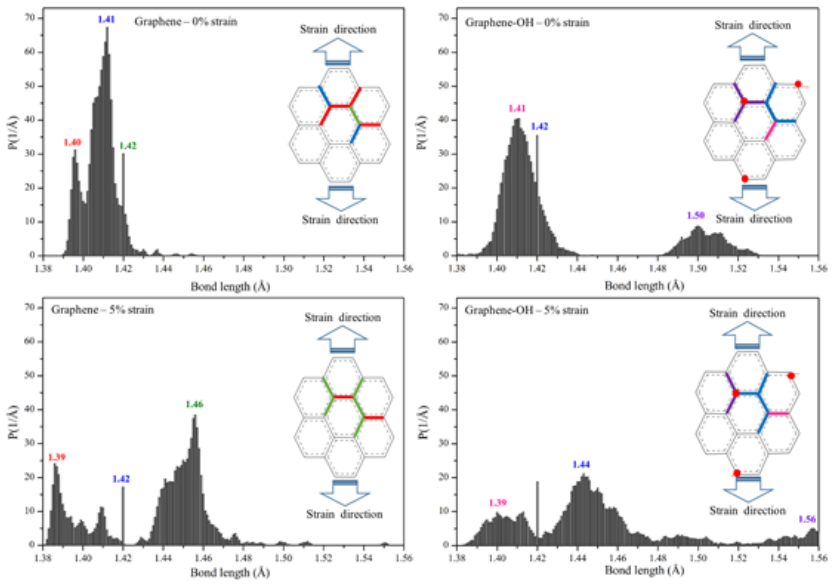


**Figure 10:** Bond length distribution plots of pristine and OH-functionalized graphene systems at 0% and 5% strain. Colors of bonds in the graphene structure relates to the colors on the distribution plot. Red dots indicate grafting sites.

As in Figure 10, the red dots present on the OH-functionalized graphene systems of Figure 11 indicate the grafting sites and the angles are colored according to the distribution plots. On the top left Figure that relates to pristine graphene without applied strain, two distinct peaks are presented at 119 ºand at 122 º. With increasing strain the angle distribution curve becomes broader and the maximum values can be predominantly found at 117 ºand 127 º. The predominance of lower angles is in connected with an increase in bond distance as a consequence of the straining, as discussed above. The OH-functionalized graphene system

with no applied strain has a different angle distribution plot with two distinct curves, a more intense with maximum at 120 ºand another at 114 º. The lower angle values include a carbon atom attached to a functional group which results in the pull-out displacement of that atom hence lower angles. The higher angle values are related to the non-functionalized carbon atoms. By applying strain, the angle distribution becomes broader and the angles which are affected by the strain direction decrease from 120 ºto 118 º.

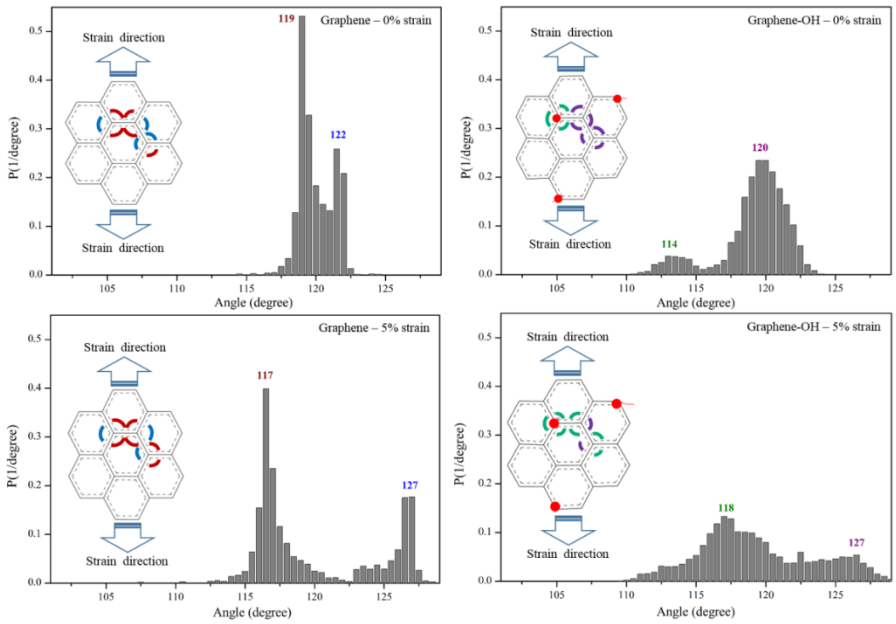


**Figure 11:** Bond angle distribution plots of pristine and OH-functionalized graphene systems at 0% and 5% strain. Colors of bonds in the graphene structure relates to the colors on the distribution plot. Red dots indicate grafting sites.

### *3.2 Young's modulus*

As described previously, the Young's modulus was determined from the strain energy vs. strain curves obtained for the pristine and the functionalized graphene systems. These curves are presented in Figure 12.

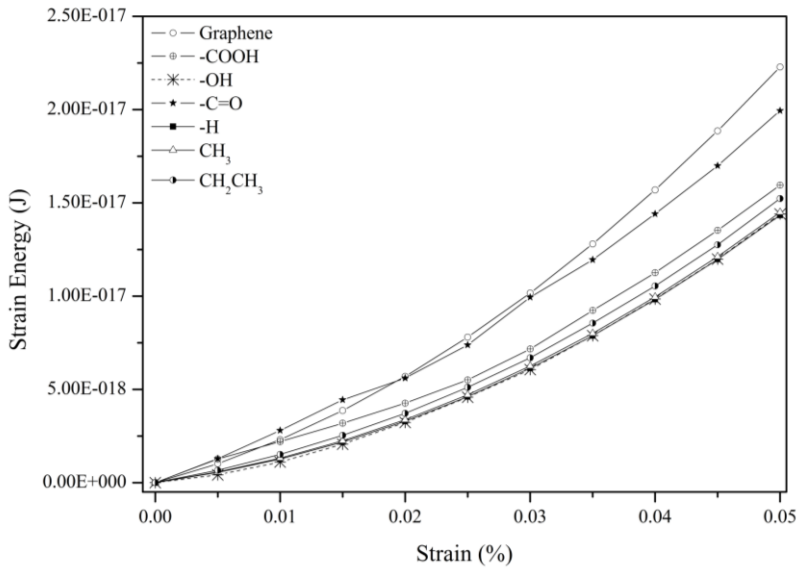


**Figure 12:** Strain energy vs. strain curves for pristine and functionalized graphene systems.

The Young's modulus of the different graphene systems are presented in Figure 13. Due to the $sp^2$-hybridized structure, pristine graphene obtained the highest value for Young's modulus, 1.18 TPa. This value is close to what is reported in the literature for MD. In the work by Tsai and Tu (2010) they present a value of 0.912 TPa for a single graphene layer. Jing, Xue, Ling, Shan, Zhang, Zhou and Jiao (2012) achieved a value of Young's modulus of 1.03 TPa, and Cho, Luo and Daniel (2007) obtained 1.15 TPa. Experimentally, and using atomic force microscope nanoidentation, Lee, Wei, Kysar and Hone (2008) obtained 1.0 TPa and Zhang and Pan (2012) reported 0.890 TPa. From our results, it is obvious that the grafting of functional groups on the graphene layer has influence on its mechanical properties. Both carboxyl and hydroxyl groups reduce the Young's modulus of graphene about 28% (0.847 TPa) and 21% (0.932 TPa), respectively. Methyl and ethyl groups decrease the modulus by approximately 25% (0.898 TPa and 0.883 TPa). Hydrogen coverage has a similar effect as methyl groups, 0.907 TPa.

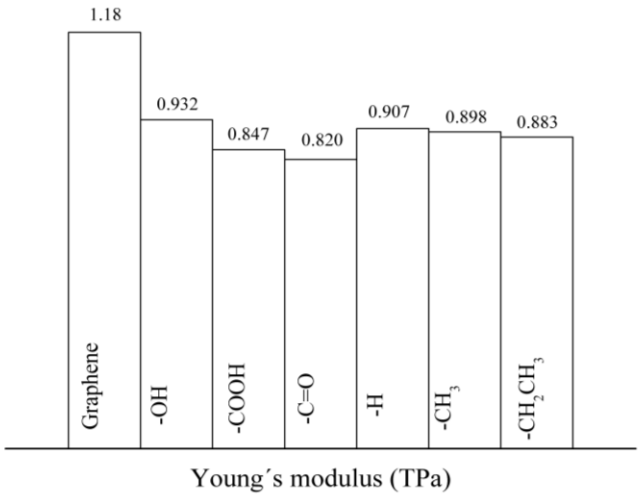


**Figure 13:** Young's modulus obtained from molecular dynamics simulations of graphene layers with functional groups.

The presence of these functional groups implies that the trigonal hybridized carbon atoms resulting from the aromaticity of pristine graphene, change to a $sp^3$-hybridization to promote the chemical adhesion. This change from in-plane geometry to out-of-plane tetrahedral geometry allows a larger rotation of the carbon due to unsupported $sp^3$ bonds. The grafted carbon buckles off-plane in course of pyramidalization as shown in Figure 14, resulting in a drop of stiffness [Pei, Zhang and Shenoy (2010b); Montazeri, Ebrahimi and Rafii-Tabar (2015)]. The effects of functionalization on the graphene structure can also be seen in Figures 10 and 11. Figure 11 in particular shows higher bond lengths for the bonds connecting a functionalized carbon and a non-functionalized as compared to pristine graphene.

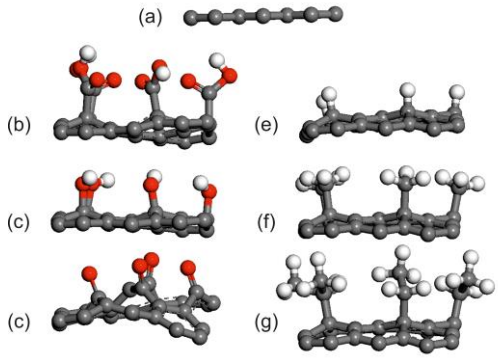


**Figure 14:** Physical conformation after geometry optimization of (a) graphene, (b) graphene-COOH, (c) graphene-OH, (d) graphene-C=O, (e) graphene-H, (f) graphene-$CH_3$, and (g) graphene-$CH_2CH_3$.

Differently, the –C=O groups promote the complete breaking of a $sp^2$ bond between one neighbor atom of the grafted carbon (see Figure 1). This vacancy defect induces a decrease of 30% (0.820 TPa) of the Young's modulus compared to pristine graphene, resulting in the lowest value for all the functional groups studied here with a 10% dispersion. Changes in the carbonyl system can be seen in Figure 14 that shows more intense out-of-plane deformations than for example the hydroxylated system. Non-functionalization induced vacancy defects have been studied previously with the AIREBO potential in MD simulations [Dewapriya and Rajapakse (2014)], and proved a decrease of ~50% in strength of graphene with 2.0% vacancy concentration indicating that vacancy defects have a major influence on the overall mechanical properties of graphene.

By grafting 10% of -OH groups differently onto 5 separate graphene models we verified that the position of the chemical groups on the layers results in a minimum variation on the Young's modulus as long as the percentage is the same.

The influence of the coverage density was studied for 3, 5, 7 and 10% grafted hydroxyl groups. Results presented in Figure 15 show a decrease of the Young's modulus with increasing degree of functionalization. This decrease of Young's modulus is expected because of the increase of $sp^3$-hybridized carbon atoms and changes of bond length and angle distribution, as discussed above, and agrees with the study by Qin and Buehler (2012) who examined the influence of the density of functional groups on the fluctuations of the graphene sheet and consequently the mechanical properties. With only 3% grafting the values drop from 1.18 TPa to 1.08 TPa, and at 5% functionalization we obtained 1.04 TPa. With 7% and 10% of functional groups distributed throughout the graphene, the decrease of Young's modulus drops to 0.906 TPa and 0.932 TPa, respectively. A similar behavior was reported by Pei, Zhang and Shenoy (2010a) who showed a slow decrease of the elastic modulus as coverage increases.

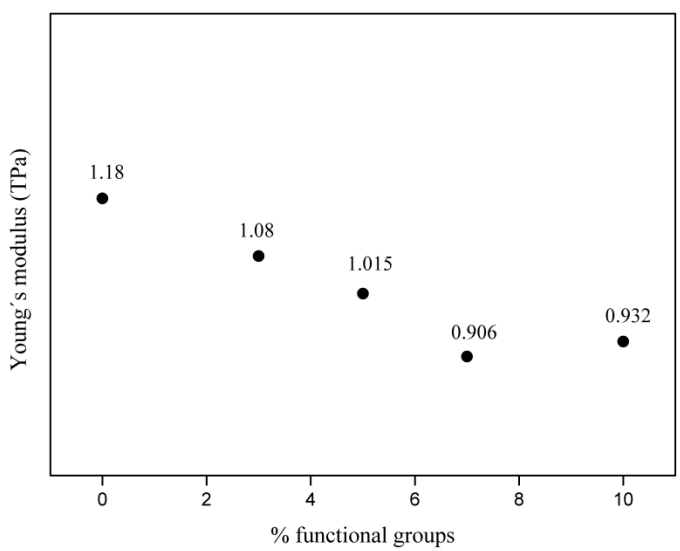


**Figure 15:** Comparison between different percentages of hydroxyl groups.

The organization of hydroxyl groups on the graphene surface has been studied for different

configurations with 3% and 10% functionalization. Comparisons between systems consisting of randomly distributed clusters and systems consisting of a single cluster were made together with systems without clusters. The 3% functionalized layers, both as a single cluster and as several clusters, showed almost no change in the Young's modulus whereas for the 10% coverage there was a drop of 20% for the single cluster (0.943 TPa) and 26% (0.867 TPa) for the several clusters. The single cluster has a higher impact on a specific area of the surface given the concentration of oxygen atoms pulling the carbon atoms away from their stable in-plane configuration, as can be seen in Figure 17. However, the several clusters have the largest impact as the distribution influences the whole structure and not a specific area. It is important to mention that these results are very much dependent on the size of the models studied. The influence of the grafting density of functional groups on the graphene properties has been previously studied by Pei, Zhang and Shenoy (2010a) as they functionalized a graphene sheet with different percentages of methyl groups by aligning them in both parallel and perpendicular directions to the tension direction. It was shown that the elastic modulus of functionalized graphene is dependent on the number and distribution direction (tension direction) of functional groups. Qin and Buehler (2012) have also suggested that an increase of the density of hydroxyl groups increases the fluctuations of the carbon atoms as a result of the hydrogen bonds between the functional groups thus decreasing the Young's modulus. Notwithstanding, the remaining functional groups that do not form hydrogen bonds be-tween each other cause similar fluctuations.

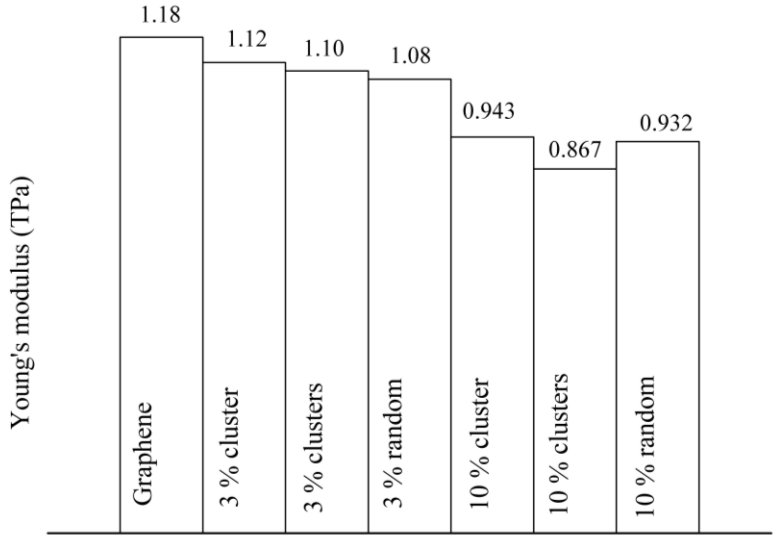


**Figure 16:** Comparison between different distributions of hydroxyl groups.

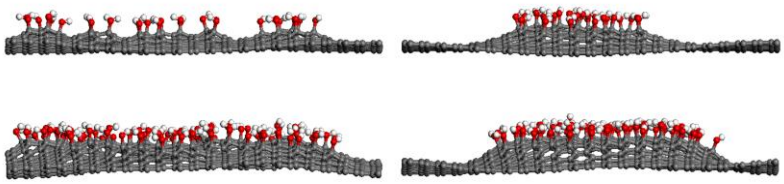

**Figure 17:** Structures with 3% (top) and 10% (bottom) of hydroxyl groups distributed as several clusters (left) and as single cluster (right) after geometry optimization.

## 4 Conclusion

The mechanical properties of graphene functionalized with carboxyl, hydroxyl, carbonyl, hydrogen, methyl, and ethyl groups were studied by calculating the modulus of elasticity. Results showed a decrease of the Young's modulus with functionalization. Hydroxylated graphene presented however the highest values obtaining 0.932 TPa, followed by hydroxyl, hydrogen, methyl, and ethyl functionalized layers, with average 0.900 TPa. Surprisingly, given the defects present on the graphene surface the carbonyl groups dropped the Young's modulus to 0.820 TPa. Grafting densities between 3% and 10% were also studied and proved a decrease on the Young's modulus with increasing functionalization. The organization of the chemical groups as a single cluster presented a higher modulus of elasticity than when organized in smaller clusters. The bond length distribution showed that the highest the degree of functionalization the broader is the distribution, meaning an increase of the graphene deformation. This factor is also dependent on the strain applied and the position of the functional groups. The distribution of the functional groups as single cluster or as several clusters does not have influence.

**Acknowledgement**: The authors would like to acknowledge the support provided by the Innovation Fund Denmark through the Danish Centre for Composites Structures and Materials for Wind Turbines grant no. 060300301B.

## References

**Accelrys Software Inc.** *Materials Studio v6.0.0.* (2011).

**Agrawal, P.M.; Sudalayandi, B.S.; Raff, L.M.; Komanduri, R.** (2006): A comparison of different methos of Young's modulus determination for single-wall carbon nanotubes (SWCNT) using molecular dynamics (MD) simulations. *Computational Materials Science*, vol. 38, pp. 271-281.

**Balandin, A.A.; Ghosh, S.; Bao, W.; Calizo, I.; Teweldebrhan, D.; Miao, F.; Lau, C.N.** (2008): Superior thermal conductivity of single-layer graphene. *Nano Letters*, vol. 8, pp. 902-907.

**Castro Neto, A.H.; Guinea, F.; Peres, N.M.R.; Novoselov, K.S.; Geim, A.K.** (2009) : The electronic properties of graphene. *Reviews of Modern Physics*, vol. 81, pp. 109-162.

**Chang, T.; Gao, H.** (2003): Size-dependent elastic properties of a single-walled carbon nanotube via a molecular mechanics model. *Journal of the Mechanics and Physics of Solids*, vol. 51, pp. 1059-1074.

**Cho, J., Luo, J.J.; Daniel, I.M.** (2007): Mechanical characterization of graphite/epoxy nanocomposites by multi-scale analysis. *Composites Science and Technology*, vol. 67, pp. 2399-2407.

**Das, D.K.; Ghosh, M.M.** (2017): On Mechanical Properties of Graphene Sheet Estimated Using Molecular Dynamics Simulations. *Journal of Materials Engineering and Performance*, vol. 26, pp. 4522-4532.

**Devanathan, R.; Chase-Woods, D.; Shin, Y.; Gotthold, W.** (2017): Molecular Dynamics Simulations Reveal that Water Diffusion between Graphene Oxide Layers is Slow. *Scientific Reports*, vol. 6, pp. 1-8.

**Dewapriya, M.A.N.; Rajapakse, R.K.N.D.** (2014): Molecular dynamics simulations and continuum modeling of temperature and strain rate dependent fracture strength of graphene with vacancy defects. *Journal of Applied Mechanics*, vol. 81, pp. 081010.

**Guo, C.Y.; Montgomery Pettitt, B.; Wheeler, L.T.** (2006): Force field comparisons of the heat capacity of carbon nanotubes. *Molecular Simulation*, vol. 32, pp. 839-848.

**Hou, Y.; Zhu, Y.B.; Liu, X.Y.; Dai, Z.H.; Liu, L.Q.; Wu, H.A.; Zhang, Z.** (2017): Elastic-plastic properties of graphene engineered by oxygen functional groups. *Journal of Physics D: Applied Physics*, vol. 50, pp. 1-10.

**Javvajia, B.; Budarapub, P.R.; Sutrakarc, V.K.; Roy Mahapatraa. D.; Paggi, M.; Zi, G.; Rabczukef, T.** (2016): Mechanical properties of Graphene: Molecular dynamics simulations correlated to continuum based scaling laws. *Computational Materials Science*, vol. 125, pp. 319-327.

**Jing, N.; Xue, Q.; Ling, C.; Shan, M.; Zhang, T.; Zhou, X.; Jiao, Z.** (2012): Effect of defects on young's modulus of graphene sheets: A molecular dynamics simulation. *RSC Advances*, vol. 2, pp. 9124-9129.

**Lee, C.; Wei, X.; Kysar, J.W.; Hone, J.** (2008): Measurement of the elastic properties and intrinsic strength of monolayer graphene. *Science*, vol. 321, pp. 385-388.

**Lin, Y.; Ding, F.; Yakobson, B.I.** (2008): Hydrogen storage by spillover on graphene as a phase nucleation process. *Physical Review B*, vol. 78, pp. 041402(R).

**Liu, X.; Yang, Q.** (2017): Molecular dynamic simulation of mechanical behavior of RGO produced by thermal reduction method. *Micro & Nano Letters*, vol. 12, pp. 638-642.

**Lv, C.; Xue, Q.; Xia, D.; Ma, M.; Xie, J.; Chen, H.** (2010): Effect of chemisorption on the interfacial bonding characteristics of Graphene-Polymer composites. *Journal of Physical Chemistry C*, vol. 114, pp. 6588-6594.

**Montazeri, A.; Ebrahimi, S.; Rafii-Tabar, H.** (2015): A molecular dynamics investigation of buckling behaviour of hydrogenated graphene. *Molecular Simulation*, vol. 41, pp. 1212-1228.

**Pei, Q.X.; Zhang, Y.W.; Shenoy, V.B.** (2010a): Mechanical properties of methyl functionalized graphene: A molecular dynamics study. *Nanotechnology*, vol. 21, pp. 115709.

**Pei, Q.X.; Zhang, Y.W.; Shenoy VB.** (2010b): A molecular dynamics study of the mechanical properties of hydrogen functionalized graphene. *Carbon*, vol. 48, pp.898-904.

**Qin, Z.; Buehler, M.** (2012): Bioinspired design of functionalised graphene. *Molecular Simulation*, vol. 38, pp. 695-703.

**Ramanathan, T.; Abdala, A.A.; Stankovich, S.; Dikin, D.A.; Herrera-Alonso, M.; Piner, R.D.; Adamson, D.H.; Schniepp, H.C.; Chen, X.; Ruoff, R.S.; Nguyen, S.T.; Aksay, I.A.; Prud'Homme, R.K.; Brinson, L.C.** (2008): Functionalized graphene sheets for polymer nanocomposites. *Nature Nanotechnology*, vol. 3, pp. 327-331.

**Sun, H.** (1998): COMPASS: An ab initio force-field optimized for condensed-phase Applications-Overview with details on alkane and benzene compounds. *Journal of Physical Chemistry B*, vol. 102, pp. 7338-7364.

**Tsai, J.; Tu, J.** (2010): Characterizing mechanical properties of graphite using molecular dynamics simulation. *Materials & Design*, vol. 31, pp. 194-199.

**Van Lier, G.; Van Alsenoy, C.; Van Doren, V.; Geerlings, P.** (2000): Ab initio study of the elastic properties of single-walled carbon nanotubes and graphene. *Chemical Physics Letters*, vol. 326, pp. 181-185.

**Xie, G.Q.; Wang, J.P.; Zhang, Q.L.** (2015): Small-Scale Effect on the Static Deflection of a Clamped Graphene Sheet. *Computers, Materials and Continua*, vol. 48, pp. 103-117.

**Yu, C.; Chen, K.; Cheng, H.; Chen, W.** (2016): A study of mechanical properties of multi-layered graphene using modified Nosé-Hoover based molecular dynamics. *Computational Materials Science*, vol. 117, pp. 127-13.

**Yu, S., Yang, S.; Cho, M.** (2009): Multi-scale modeling of cross-linked epoxy nanocomposites. *Polymer*, vol. 50, pp. 945-952.

**Zhang, C.; Hao, X.-L.; Wang, C.-X.; Ning, W.; Rabczuk, T.** (2017): Thermal conductivity of graphene nanoribbons under shear deformation: A molecular dynamics simulation. *Scientific Reports*, vol. 7, pp. 1-8.

**Zhang, Y.; Pan, C.** (2012): Measurements of mechanical properties and number of layers of graphene from nano-indentation. *Diamond and Related Materials*, vol. 24, pp. 1-5.

**Zheng, Q.; Geng, Y.; Wang, S.; Li, Z.; Kim, J.** (2010): Effects of functional groups on the mechanical and wrinkling properties of graphene sheets. *Carbon*, vol. 48, pp. 4315-4322.

**Zhou, L., Xue, J., Wang, Y.; Cao, G.** (2013): Molecular mechanics simulations of the deformation mechanism of graphene monolayer under free standing indentation. *Carbon*, vol. 63, pp. 117-124.

**Zhou, L.; Wang, Y.F.; Cao, G.** (2013): Elastic properties of monolayer graphene with different chiralities, *Journal of Physics: Condensed Matter*, vol. 25, pp. 125302.